

Changes in the Melting Temperature and Crystal Structure of Poly(Vinylidene Fluoride) by Knotting

Yasuhiro Matsuda, Yuya Ota, Shigeru Tasaka

Department of Materials Science and Chemical Engineering, Shizuoka University, 3-5-1 Johoku, Naka-Ku, Hamamatsu, 432-8561, Japan

Correspondence to: Y. Matsuda (E-mail: tymatud@ipc.shizuoka.ac.jp)

ABSTRACT: A significant increase in the melting temperature of knotted fibers of poly(vinylidene fluoride) (PVDF) was detected by differential scanning calorimetry. The melting peak partially returned to the original peak after the fibers were unknotted. Knotted PVDF fibers were observed with an optical microscope at crossed-nicol conditions. The knotted portions of the fibers showed birefringence even above the melting temperature of the fibers before knotting. The dependence of the physical properties of PVDF under applied stress was estimated in order to investigate the influence of knotting. The fracture temperature of PVDF fibers increased with applied stress below 1 MPa and decreased above 10 MPa because the applied stress increased the melting temperature of PVDF crystals, but strong stress mechanically broke the fibers. The X-ray diffraction patterns of the PVDF fibers under different stress were divided into the peaks of α - and β -phase crystals and amorphous. The peak area of the β -phase crystal increased and that of the amorphous decreased with applied stress. © 2012 Wiley Periodicals, Inc. *J. Appl. Polym. Sci.* 000: 000–000, 2012

KEYWORDS: crystallization; differential scanning calorimetry; X-ray

Received 19 April 2012; accepted 19 August 2012; published online

DOI: 10.1002/app.38493

INTRODUCTION

Weaving fibers into cloth inevitably tangles fibers together. The stress induced by the entanglement of the fibers can change their physical properties, such as the increase in the melting temperature, which raises the mechanical strength of the fibers. The dependence of phase transition temperature on applied pressure can be predicted by the Clausius-Clapeyron equation, as follows:

$$\left(\frac{\partial P}{\partial T}\right)_{\text{eq}} = \frac{\Delta H}{T\Delta V} \quad (1)$$

where P , T , H , and V stand for pressure, temperature, enthalpy, and volume, respectively, and the subscript “eq” indicates equilibrium conditions.

There have been many researches on the changes in melting temperatures induced by pressure, and the increase in the melting temperatures of fibers at 100 MPa were reported to be 20°C for nylon 6,¹ 70°C for poly(ethylene tetrafluoroethylene),² 11–13°C for polypropylene,³ 20°C for low-density-polyethylene,⁴ and 16°C for high-density-polyethylene.⁵

In this study, we prepared knotted poly(vinylidene fluoride) (PVDF) fibers and detected a significant increase in their melt-

ing temperature by differential scanning calorimetry (DSC). Using Clausius-Clapeyron equation and the ΔV reported by Santos et al.⁶ the relation between the increase in the melting temperature of PVDF and pressure can be approximated as $\Delta T = 0.170 P$, where the units of T and P are °C and MPa, respectively. The increase in melting temperature induced by knotting was much greater than that estimated by the Clausius-Clapeyron equation, and it was suggested that some structural changes in the PVDF crystals induced by the stress of knotting might increase the melting temperature.

It is known that there are at least four crystal forms of PVDF: α , β , γ and δ phases.^{7–10} PVDF forms mainly α -phase crystals in films prepared by melt pressing or solution casting, but the α -phase crystals can be transformed into β -phase crystals by mechanical deformations such as stretching.¹¹

There have been many researches on the changes of the crystal structure induced by mechanical deformation. Du et al.¹² carried out X-ray diffraction (XRD) and small and wide angle X-ray scattering measurements for the PVDF fibers stretched at various temperatures and stretching rates and ratios. They confirmed the transition of crystal structure from α - to β -phase, and estimated the relation between the stretching conditions and the change of the crystal structure.

Lund and Hagström¹¹ prepared PVDF fibers by melt-spinning and drawing and measured the melting behavior and stress-strain curves in addition to XRD. They discussed the melting behavior of their fibers prepared by melt-spinning and drawing based on the change of the crystal structure from α - to β -phase estimated by the XRD.

As mentioned above, we detected a significant increase in the melting temperature of PVDF fibers induced by knotting. To estimate the influence of the applied stress induced by knotting on the crystallization behavior of fibers of PVDF, XRD was carried out for the PVDF fibers under stress. The XRD patterns were separated into peaks of crystals and amorphous regions, and the changes in crystal structure induced by the applied stress were discussed to explain the increase in the melting temperature.

EXPERIMENTAL

All the PVDF fibers used in this study were products of Kureha Gosen. Fibers with different diameters were used in this study, but the data for the fibers with a diameter of 64 μm (#1100) are shown in this article, unless the diameter of the sample is otherwise described.

PVDF pellets purchased from Aldrich with weight average molecular weight of 530,000 were also used for DSC measurements in order to estimate the influence of crystallinity on the melting behavior. The crystallinity of these pellets is lower than that of the fiber samples supplied from Kureha Gosen, because the polymer chains in these pellets contain more head-to-head and tail-to-tail bonds than those in the sample supplied from Kureha Gosen. The PVDF films made by hot-pressing the pellets were cut into strips, and were stretched to prepared PVDF fibers.

Although we investigated various conditions to knot fibers, only the data for 100 filaments of PVDF knotted by applying 1.0 kg by overhand knot are shown in this paper, unless otherwise described. The shape of the DSC curve of knotted fibers was essentially independent of the applied force above 0.2 kg, and the number of knotted filaments between 100 and 1000 filaments. DSC was also carried out for fibers knotted by fisherman's knot, but there were no obvious difference between the fibers knotted by overhand knot. The DSC measurements were carried out with a DSC-60 instrument from Shimadzu. The heating rate was fixed at 20°C/min. About 1 mg of the samples were put into aluminum pans, and measured under nitrogen atmosphere (100 ml/min). The temperature was calibrated with the melting temperature of indium.

Optical micrographs were taken with a Labpho-Pol from Nikon equipped with a hot stage. Fibers were observed at crossed-nicol conditions with 100 \times magnification. One end of the fiber was fixed, and the other end was tied to a weight to apply stress. The applied stress was calculated from the diameter of a fiber measured by an optical micrograph assuming that the cross section of the fiber is a circle.

The fracture temperature of PVDF was measured by applying different stresses in a constant temperature oven (DN43H,

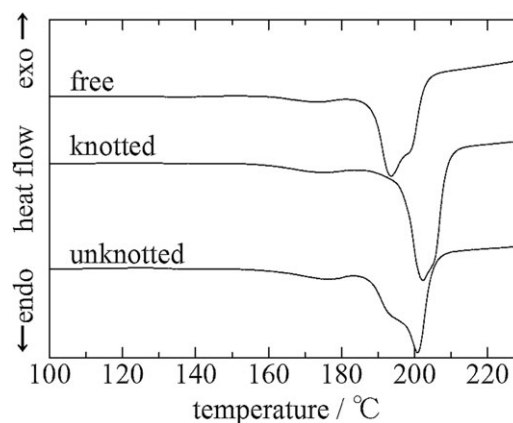


Figure 1. The DSC curves of PVDF fibers. “Knotted” and “free” indicate the results for fibers with and without knotting. “Unknotted” fibers were first knotted, and then unknotted before the measurement.

Yamato Scientific) heating at 5°C/min. Both ends of a sample fiber were tied to aramid fibers. One aramid fiber was fixed, and the other fiber was tied to a weight.

The PVDF fibers were wound to an aluminum plate by applying different stresses to prepare samples for XRD measurements, which were conducted with a RINT 2200 X-ray diffractometer from Rigaku using $\text{CuK}\alpha$ radiation with wavelength of 0.154 nm as the X-ray source. The voltage and current of the X-ray tube were 40 kV and 40 mA, respectively. The intensity of the diffracted X-ray was scanned at a rate of 4.0°/min at room temperature.

RESULTS

Figure 1 shows the DSC curves of the PVDF fibers, where “knotted” and “free” indicate the results for fibers after and before knotting. Fibers defined as “unknotted” were first knotted and then unknotted before the measurement. The melting temperature of the PVDF fibers increased by $\sim 10^\circ\text{C}$ after knotting.

If this increase had been caused purely by the applied pressure, the Clausius-Clapeyron equation would predict the applied pressure to be 60 MPa, which is an unrealistically high pressure for a knot. We also knotted other fibers, such as polypropylene, polyethylene terephthalate, and nylon 6 in the same procedure, but the increases of their melting temperatures were less than 2°C. These results suggest that structural change of the PVDF fibers induced by knotting increased its melting temperature.

The DSC curve of the unknotted PVDF has a broad endothermic peak around the melting temperatures of free and knotted fibers. This result indicates that the unknotted PVDF only partially reversed to the original structure.

To confirm the increase in the melting temperature induced by knotting, optical microscopy at crossed-nicol condition was carried out for the knotted fibers. Optical micrographs of the knotted fibers were taken by heating as shown in Figure 2. While the entire fiber appeared bright at 120°C, only the knotted portion of the fiber can be seen at 170°C, and the other portions

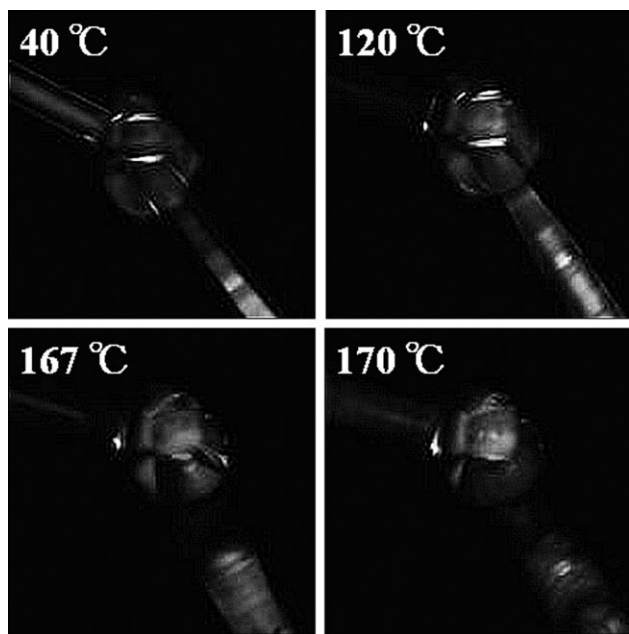


Figure 2. Optical micrographs of knotted fiber at crossed-nicol condition. The micrographs were taken by heating on a hot plate.

were dark. This result indicates that the crystals in the knotted portion melted at higher temperature than those in other portions. This behavior supports the results of DSC, which indicated that the increase in the melting temperature was induced by knotting.

The dependence of the melting temperature of PVDF fibers on the diameter of the filaments and the stress applied to the fibers is shown in Figures 3 and 4. The melting temperature of PVDF fibers with a diameter of 39 μm was $\sim 20^\circ\text{C}$ higher than that of the fibers with larger diameters. However, no clear relation between the melting temperature increases induced by knotting and their diameters was observed for the fibers used in this study. The melting temperature was almost independent of the weight used to apply stress between 1 and 4 kg.

To investigate the dependence of crystallinity on the melting behavior of PVDF, DSC curves of PVDF fibers with lower crys-

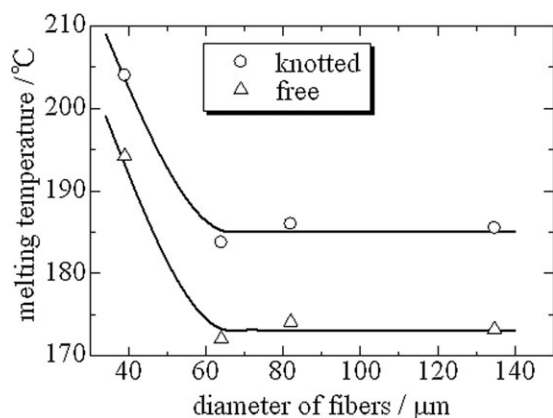


Figure 3. Melting temperature of knotted PVDF fibers with various diameters.

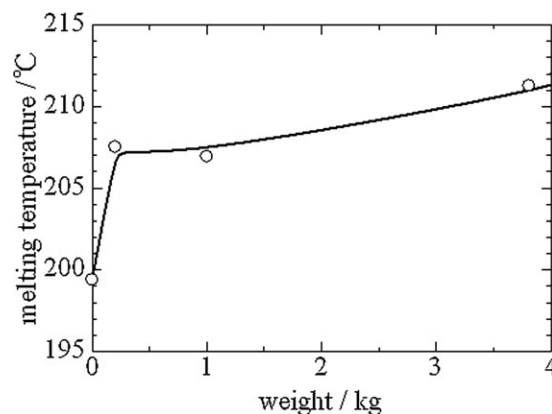


Figure 4. Melting temperature of PVDF fibers knotted using different weights.

tallinity were measured as shown in Figure 5. The heat of fusion of the sample purchased from Aldrich was lower than that of the sample supplied from Kureha Gosen, which indicated the former sample had lower crystallinity. Knotting increased the melting temperature of the fibers with a higher crystallinity by about 30°C . However, the increase in the melting temperature of the fibers with lower crystallinity was only 2°C , which can be explained by the Clausius-Clapeyron equation. These results indicate that high crystallinity is necessary for the drastic increase in melting temperature by knotting.

To elucidate the dependence of melting behavior on the stress applied to fibers, the fracture temperature of PVDF fibers was determined by applying different weights. The fracture temperature of PVDF fibers slowly increased with applied stress below 1 MPa, and decreased above 10 MPa as shown in Figure 6. The increase in the fracture temperature can be explained by the increase in the melting temperature of the PVDF crystals induced by the applied stress. The decrease in the fracture temperature above 10 MPa does not necessarily imply the decrease in the melting temperature, because high stress applied to fibers

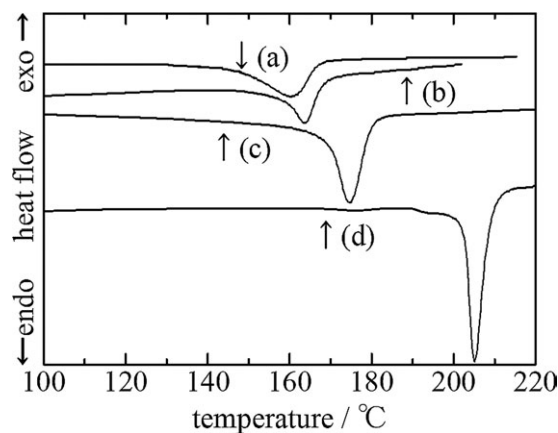


Figure 5. The DSC curves of PVDF fibers. (a) free fibers comprised of PVDF with low crystallinity, (b) knotted fibers comprised of PVDF with low crystallinity, (c) free fibers comprised of PVDF with high crystallinity, and (d) knotted fibers comprised of PVDF with high crystallinity.

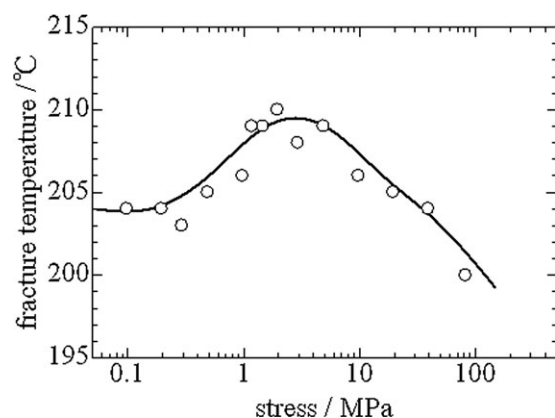


Figure 6. Fracture temperature of PVDF fibers applied different stresses.

mechanically fracture weak fibers just below their melting temperature.

The birefringence of PVDF fibers under various stresses and temperatures was calculated from the color of the optical micrographs obtained at crossed-nicol conditions. The data at 16 and 41 MPa shown in Figure 7 are shifted vertically in order to show the data clearly. The birefringence of fibers with higher applied stress decreased at higher temperatures, which indicates that the crystals induced by higher stress had higher melting temperature.

The XRD measurements were carried out to elucidate the crystal structure of PVDF under stress. Figure 8 illustrates the XRD patterns of the PVDF fibers with a diameter of $39\ \mu\text{m}$ under different stress conditions. The peak angles of XRD patterns of PVDF crystals assigned by Du et al.¹² are depicted with broken lines in the figure. The intensities of the peaks assigned to α -phase crystals decreased, but those assigned to β -phase crystals slightly increased with applied stress.

To estimate the details of the crystal structure, the obtained patterns were divided into three peaks for the α -phase crystals, one peak of β -phase crystal, and broad amorphous peak assuming

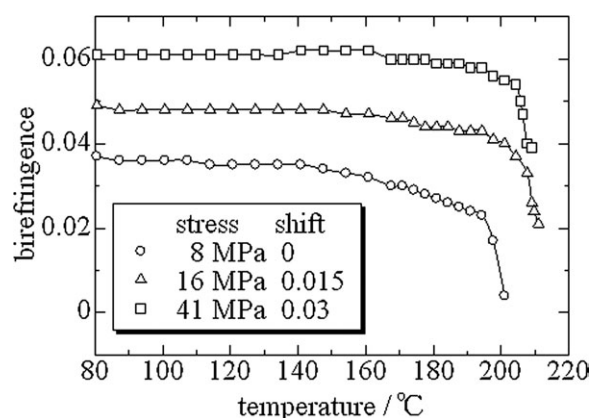


Figure 7. Temperature dependence of birefringence of PVDF fibers under applied stresses. The data points are vertically shifted as indicated in the figure.

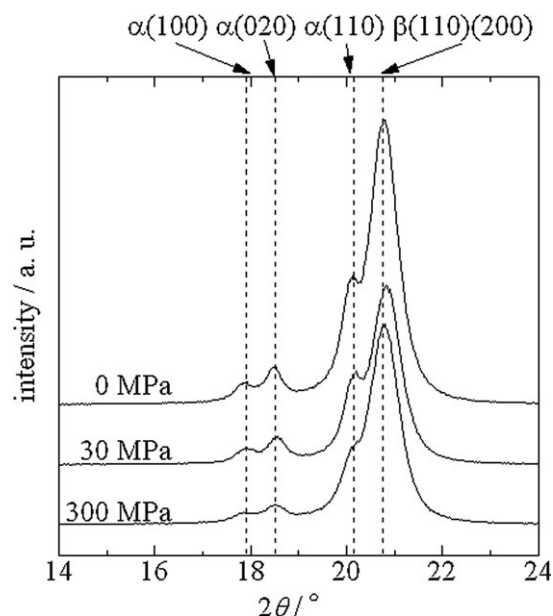


Figure 8. XRD patterns of PVDF fibers with diameter of $39\ \mu\text{m}$ under different stress. Broken lines indicate the peak angles of XRD patterns of PVDF crystals reported by Du et al.

Gaussian distributions. Figure 9 shows a typical XRD pattern and separated peaks assigned as shown in Figure 8.

The small residual deviation shown in Figure 9 suggests that the obtained peaks were successfully separated into the assigned peaks. The other XRD patterns were also successfully divided into peaks of α - and β -phase crystals and amorphous. The changes in the peak area ratios and full width at half maximum (FWHM), that fit the experimental data best, are shown in Figure 10. The peak area ratio of the β -phase crystals increases in

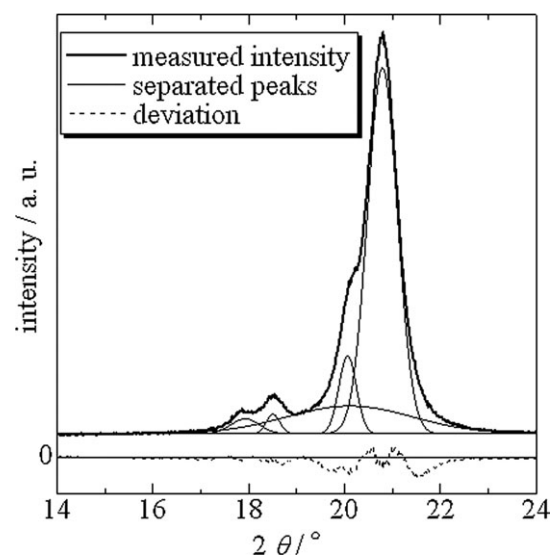


Figure 9. A typical XRD pattern and separated peaks. Thick and thin lines indicate the measured pattern, and separated peaks assigned as shown in Figure 8, respectively. Broken line illustrates the residual deviation.

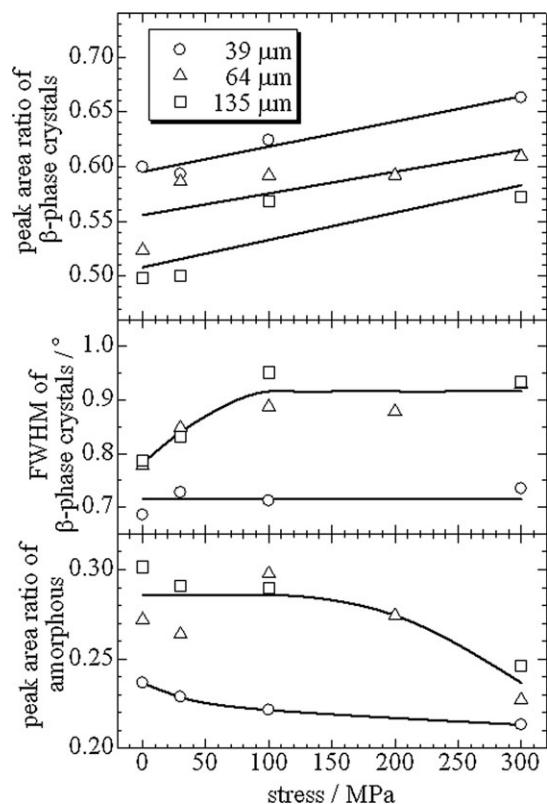


Figure 10. Parameters determined by fitting XRD patterns measured for fibers with different diameters under different stress.

fibers with smaller diameter under higher stress. The peak of β -phase crystals in the fibers with diameters of 39 μm was independent of the applied stress. However, those in the fibers with diameters of 64 and 135 μm became broader between 0 and 100 MPa, and constant between 100 and 300 MPa. The peak ratio of the amorphous regions decreased slightly with applied stress in the fibers with diameter of 39 μm , and those in the fibers with diameters of 64 and 135 μm decreased more steeply between 100 and 300 MPa.

DISCUSSION

Figures 1 and 2 clearly show a significant increase in the melting temperature of PVDF crystals induced by knotting. The fracture temperatures in Figure 6 and the temperature dependence of birefringence in Figure 7 indicate the increase in melting temperature of PVDF crystals induced by applied stress. Considering these results, the melting temperature of PVDF fibers can be drastically increased by applying stress such as knotting the fibers.

The change in the crystal structure of PVDF induced by stress was analyzed by XRD. For the fibers with diameters of 64 and 135 μm , the peak area of the β -phase crystals increased, and those of the α -phase crystals and amorphous decreased, but the peak of the β -phase crystals became broader under applied stress. The results of XRD suggest that the α -phase crystals and the amorphous regions were changed into β -phase crystals, but the quality of the β -phase crystals was not high, and there were

many defects in the β -phase crystals induced by the applied stress. It has been reported that the β -crystals of PVDF have higher melting temperature than α -crystals.^{13–15} The highly orientated β -crystals of PVDF may play important roles in the increase in the melting temperature of PVDF, although more detailed mechanism of the increase in the melting temperature should be clarified in the future study.

The independence of the melting temperature of knotted fibers and the dependence of the crystal structure of PVDF on the applied stress seem to be contradictory at first sight. While the fibers were being knotted, the weights gave stress to the fibers. However, the weights were removed after knotting. Some stress at the knots remained after the removal of the knots, but the knots might be unable to maintain the strong stress, and allow the relaxation of the strong stress. On the other hand, the fibers were kept being stretched by being wound to an aluminum plate.

Three fibers with different diameters were used in this study, and some differences were detected between the fibers with a diameter of 39 μm and those with diameters of 64 and 139 μm as shown in Figures 3 and 10. The fibers with small diameters are strongly drawn during their fabrication. The strong elongation stretching the polymer chains in fibers can change the melting behavior of the polymer chains.^{16,17}

The elevated melting temperature of fibers with small diameters was also reported by Lund et al.¹¹ They spun PVDF fibers with different melt draw ratios, and measured their melting behavior by DSC. Whereas there were no distinct differences between the DSC curves of the fibers with different melt draw ratios of 42 and 84, a melting peak appeared $\sim 20^\circ\text{C}$ higher than the original melting peak of the fibers with melt draw ratios of 251.

CONCLUSIONS

The increase in the melting temperature of poly(vinylidene fluoride) (PVDF) fibers by knotting was measured by DSC and optical microscopy under crossed-nicol conditions. The melting temperature of the PVDF fibers with high crystallinity was increased $\sim 10^\circ\text{C}$ by knotting, which cannot be explained solely by the effect of applied pressure on the melting temperature in the Clausius-Clapeyron equation.

The DSC measurements for the PVDF fibers with different crystallinity indicate that high crystallinity is indispensable to the increase in the melting temperature induced by knotting. The XRD patterns showed that high stress to the fibers induced the increase in β -crystals and decrease in amorphous structure, which may contribute the increase in the melting temperature by knotting.

This change in the melting temperature and crystal structure influence the physical properties of PVDF fibers. The fracture temperature of PVDF fibers increased by applying stress below 1 MPa, while it decreased above 10 MPa, for the applied stress broke the fibers mechanically. Although the detailed mechanism of the increase in the melting temperature should be elucidated in future study, the results in this paper indicate that knotting

can play important roles in some practical properties of PVDF fibers.

ACKNOWLEDGMENTS

PVDF fibers used in this study were kindly supplied from Kureha Gosen. This work is partially supported by a Grant-in Aid for Young Scientists (B) (23700869) from the Ministry of Education, Culture, Science, Sports and Technology of Japan.

REFERENCES

1. Kojima, Y.; Takahara, M.; Matsuoka, T.; Takahashi, H. *J. Appl. Polym. Sci.* **2001**, *80*, 1046.
2. Nakafuku, C.; Takaoka, K.; Katsura, K. *Polym. J.* **1999**, *31*, 557.
3. Seeger, A.; Freitag, D.; Freidel, F.; Luft, G. *Thermochim. Acta* **2004**, *424*, 175.
4. Höhne, G. W. H. *Thermochim. Acta* **1999**, *332*, 115.
5. Nakafuku, C.; Nakagawa, H.; Yasuniwa, M.; Tsubakihara, S. *Polymer* **1991**, *32*, 696.
6. Santos, W. N.; Iguchi, C. Y.; Gregorio, R., Jr. *Polym. Test.* **2008**, *27*, 204.
7. Takahashi, Y.; Matsubara, Y.; Tadokoro, H. *Macromolecules* **1983**, *16*, 1588.
8. Carbeck, J. D.; Rutledge, G. C. *Polymer* **1996**, *37*, 5089.
9. Schwartz, M., Ed. *Encyclopedia of Smart Materials*; Wiley: New York, **2002**.
10. Hasegawa, R.; Takahashi, Y.; Chatani, Y.; Tadokoro, H. *Polym. J.* **1972**, *3*, 600.
11. Lund, A.; Hagström, B. *J. Appl. Polym. Sci.* **2010**, *116*, 2685.
12. Du, C.; Zhu, B.-K. Xu, Y.-Y. *J. Appl. Polym. Sci.* **2007**, *104*, 2254.
13. Doll, W. W.; Lando, J. B. *J. Macromol. Sci. Phys.* **1968**, *B2*, 205.
14. Doll, W. W.; Lando, J. B. *J. Macromol. Sci. Phys.* **1970**, *B4*, 889.
15. Matsushige, K.; Takemura, T. *J. Polym. Sci. Polym. Phys. Ed.* **1978**, *16*, 921.
16. Vasanthan, N. *J. Polym. Sci. Part B Polym. Phys.* **2003**, *41*, 2870.
17. Shabana, H. M. *Polym. Int.* **2004**, *53*, 919.